ORIGINAL

Effects of EOS789, a novel pan-phosphate transporter inhibitor, on phosphate metabolism : Comparison with a conventional phosphate binder

Kazuya Tanifuji[1], Yuji Shiozaki[1], Megumi Koike[1], Minori Uga[1], Aoi Komiya[1], Mizuki Miura[1], Ayami Higashi[1], Takaaki Shimohata[2], Akira Takahashi[2], Noriko Ishizuka[3], Hisayoshi Hayashi[3], Yasuhiro Ichida[4], Shuichi Ohtomo[5], Naoshi Horiba[4], Ken-ichi Miyamoto[1, 6], and Hiroko Segawa[1]

[1]Department of Applied Nutrition, Tokushima University Graduate School of Biomedical Sciences, Tokushima, Japan, [2]Department of Preventive Environment and Nutrition, Tokushima University Graduate School of Biomedical Sciences, Tokushima, Japan, [3]Laboratory of Physiology School of Food and Nutritional Sciences, University of Shizuoka, Suruga-ku, Shizuoka, Japan, [4]Research Division, Chugai Pharmaceutical Co., Ltd. Yokohama, Kanagawa, Japan, [5]Translational Research Division, Chugai Pharmaceutical Co., Ltd. Research Division, Tokyo, Japan, [6]Graduate School of Agriculture, Ryukoku University, Ohtsu, Japan

Abstract : Background : Inorganic phosphate (Pi) binders are the only pharmacologic treatment approved for hyperphosphatemia. However, Pi binders induce the expression of intestinal Pi transporters and have limited effects on the inhibition of Pi transport. EOS789, a novel pan-Pi transporter inhibitor, reportedly has potent efficacy in treating hyperphosphatemia. We investigated the properties of EOS789 with comparison to a conventional Pi binder. Methods : Protein and mRNA expression levels of Pi transporters were measured in intestinal and kidney tissues from male Wistar rats fed diets supplemented with EOS789 or lanthanum carbonate (LC). ^{32}Pi permeability was measured in intestinal tissues from normal rats using a chamber. Results : Increased protein levels of NaPi-2b, an intestinal Pi transporter, and luminal Pi removal were observed in rats treated with LC but not in rats treated with EOS789. EOS789 but not LC suppressed intestinal protein levels of the Pi transporter Pit-1 and sodium/hydrogen exchanger isoform 3. ^{32}Pi flux experiments using small intestine tissues from rats demonstrated that EOS789 may affect transcellular Pi transport in addition to paracellular Pi transport. Conclusion : EOS789 has differing regulatory effects on Pi metabolism compared to LC. The properties of EOS789 may compensate for the limitations of LC therapy. The combined or selective use of EOS789 and conventional Pi binders may allow tighter control of hyperphosphatemia. J. Med. Invest. 70 : 260-270, February, 2023

Keywords **:** *hyperphosphatemia, CKD, intestine, phosphate transporter*

INTRODUCTION

Hyperphosphatemia is an independent risk factor for mortality, and treatment with phosphate (Pi) binders is independently associated with improved survival in patients with chronic kidney disease (CKD). Findings from experimental studies support previous epidemiologic findings, with clinical practice guidelines recommend in specific targets for serum Pi levels in patients requiring dialysis. As the prevention and correction of hyperphosphatemia are major goals of the treatment of CKD-mineral and bone disorder, special attention must be focused on Pi balance (1, 2).

Current strategies for treating hyperphosphatemia in patients requiring dialysis include dietary phosphorus restriction and oral Pi binders. However, if used aggressively, these treatments can lead to malnutrition, adverse gastrointestinal effects, and poor compliance with all medications, particularly in elderly patients. Furthermore, Pi binders account for a large proportion of the daily pill burden of patients requiring dialysis. The pill burden and adverse effects associated with Pi binders often contribute to poor medication adherence (2-7). Accordingly, there is a need for the development of novel small molecular compounds for the treatment of hyperphosphatemia, such as Pi transport inhibitors.

Pi absorption is thought to be mediated by transcellular transport and passive transport via paracellular transport. The Pi transporters NaPi-2b, Pit-1, and Pit-2 have been shown to localize to the luminal side of the intestinal wall and are responsible for Pi absorption in transcellular transport (8-11). Ours and other groups have previously clarified the importance of Pi transporters in intestinal Pi absorption using NaPi-2b knockout (Npt2b KO) mice (12-15). Furthermore, regulation of intestinal NaPi-2b levels may contribute to the development of CKD in Npt2b KO mice model of CKD (13-15). Accordingly, several groups are attempting to develop inhibitors of NaPi-2b as potential small molecular therapies for hyperphosphatemia (16-21). However, previous clinical trials of NaPi-2b inhibitors have reported no improvements in hyperphosphatemia (22, 23). This may be attributable to the important contribution of duodenal and jejunal Pit-2 expression to intestinal Pi absorption in humans, whereas small intestinal NaPi-2b plays a predominant role in Pi absorption in mice (24).

EOS789 is a pan-Pi transporter inhibitor with low absorption, low accumulation in the body, and potentially potent inhibition of Pi transport at low doses (2, 25-27). EOS789 interacts with several sodium-dependent phosphate transporters (NaPi-2b, Pit-1, and Pit-2) known to contribute to intestinal phosphate absorption (25-27). Furthermore, EOS789 was reported to improve hyperphosphatemia, severe glomerulosclerosis, tubular degeneration, and tubulointerstitial fibrosis and suppress vascular

Received for publication February 19, 2023 ; accepted February 27, 2023.

Address correspondence and reprint requests to Hiroko Segawa PhD, Department of Applied Nutrition, Institute of Biomedical Sciences, Tokushima University Graduate School, 3-18-15 Kuramoto-Cho, Tokushima City 770-8503, Japan and Fax : +81-88-633-7082. E-mail : segawa@tokushima-u.ac.jp

calcification in a rat model of CKD (25-27). However, the effects of EOS789 on Pi metabolism compared to conventional Pi binders remain unclear. Furthermore, the effect of EOS789 on paracellular transport of Pi has yet to be investigated.

Recent studies have elucidated the role of sodium/hydrogen exchanger isoform 3 (NHE3) and the paracellular transport system in intestinal Pi absorption. Clinical trials of tenapanor, an inhibitor of NHE3 in the gastrointestinal tract, are currently ongoing. Tenapanor has a different mechanism of action to previous Pi binders and may cause H^+ to remain in the cell and increase transepithelial resistance by inhibiting NHE3 in the gastrointestinal tract, thereby inhibiting paracellular Pi absorption (28). Tenapanor has been reported to improve hyperphosphatemia in patients receiving regular hemodialysis (29). Accordingly, paracellular Pi transport may be more important as Pi concentrations in the lumen of the gastrointestinal tract increase ; however, this mechanism remains poorly understood.

To date, the effect of EOS789 on NHE3 and paracellular Pi transport remains unclear. In the present study, the effect of EOS789 on Pi metabolism was compared to a conventional Pi binder (lanthanum carbonate ; LC). Furthermore, we investigated the effect of EOS789 on paracellular Pi transport.

MATERIAL AND METHODS

Experimental animals

Male five-week-old Wistar rats were purchased from Charles River Laboratories Japan (Yokohama, Japan). Rats were maintained under pathogen-free conditions and provided free access to water and standard rat chow CRF-1 (ORIENTAL YEAST, Tokyo, Japan). Rats were maintained under pathogenfree conditions and handled in accordance with the Guidelines for Animal Experimentation of Tokushima University School of Medicine (T29-3).

Experimental design

The present study comprised two experiments. Figure 1 presents overviews of the respective experimental designs. Rats were housed in metabolic cages and provided free access to water and standard rat chow (CRF-1). Access to chow was restricted to 10 g for five days prior to the experimental period. Body weight, plasma Pi and calcium (Ca) levels, and urinary Pi and calcium excretion were measured on the day prior to the experimental period (day -1). Rats were then divided into three groups. The Control group was fed 10 g of CRF-1 per day, the EOS789 group was fed 10 g of CRF-1 containing 0.15% of EOS789 per day, and the LC group was fed 10 g of CRF-1 containing 1.74% of LC per day for three days (days 1–3).

$^{33}PO4$ balance study

Methods for the measurement of $^{33}PO4$ balance have previously been described (26). In the present study, 100 ml of $H_3{}^{33}PO^4$ solution corresponding to 170 kBq was added to 10.0 g of powdered CRF-1 without EOS789 or LC, containing 0.50% EOS789, or containing 0.75%, 1.5%, or 3% LC. Rats were fed 10.0 g of chow containing $H_3{}^{33}PO4$ with EOS789 or LC per day for three consecutive days, followed by 10.0 g/day of powdered chow without the test drug or $H_3{}^{33}PO^4$ for two days to allow collection of feces and urine samples. A liquid scintillation counter was used to measure ^{33}P radioactivity in feces, urine, and serum samples from each rat. Total fecal or urinary ^{33}P excretion was calculated by dividing ^{33}P radioactivity in feces or urine by the total ^{33}P radioactivity in chow (26).

Blood, urine, and feces collection

Rats were individually placed in a metabolic cage to quantitfy urine and fecal collection over a 24-hr period. Tail vein blood was collected at 10:00 a.m. on the day prior to drug administration. Blood samples from the inferior vena cava were collected at the end of the experimental period. Blood samples were divided into plasma and serum. Urine samples were vortexed after the addition of an equal volume of 1N HCl and centrifuged at 3,000 rpm at 20℃ for 20 min. Supernatants were then used for further analyses. Fecal samples were collected and allowed to dry at 110℃ for no more than 24 hr. Fecal samples were then heated at 250℃ for 3 hr and at 550℃ for 24 hr in a muffle furnace. Samples were then cooled, weighed, and digested in HCl with heating. Sample volumes were standardized to 25 ml.

Biochemical measurements

Pi, Ca, and creatinine concentrations were determined using commercial kits (WAKO, Osaka, Japan). Plasma concentrations of Fibroblast growth factor (FGF) 23, parathyroid hormone (PTH), and $1,25(OH)_2D_3$ were determined using the intact FGF23 (KAINOS Laboratories), intact PTH (Immunotopics Inc.), and 1,25-$(OH)_2$ Vitamin D ELISA kits (Immundiagnostik), respectively.

Tissue sample preparation

Kidney samples were dissected in the coronal axis. Small intestine samples were dissected approximately 10 cm from the stomach pylorus. Samples were used for real-time PCR, western blotting analysis, and immunostaining.

RNA extraction and cDNA synthesis

Total RNA was extracted from mouse tissues using ISOGEN (Wako) according to the manufacturer's instructions. After

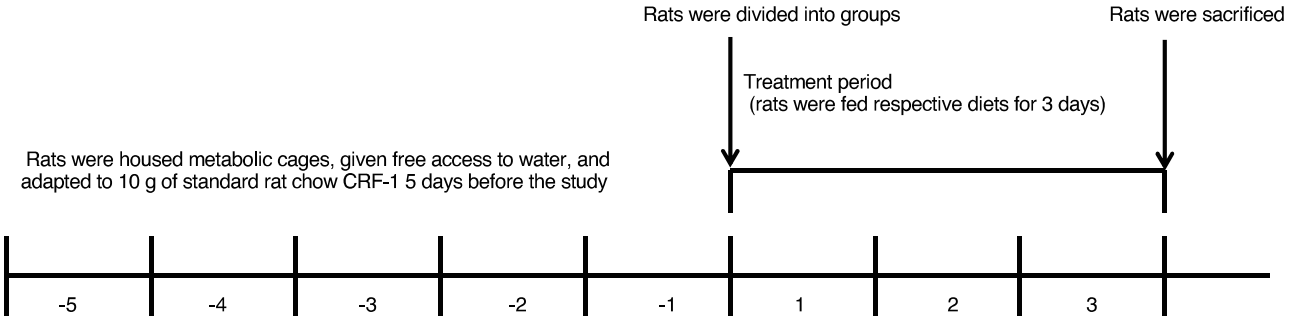

Figure 1. Drug administration schedule
Schedule of EOS789 and lanthanum carbonate administration for three days in six-week-old Wistar rats.

treatment with DNase (Invitrogen), cDNA was synthesized using reverse transcriptase (Invitrogen) and oligo(dT)12–18 primers, with, or without Moloney murine leukemia virus RNA. The PCR primer sequences used in the present study are shown in Table 1. To check for genomic DNA contamination, a reverse transcriptase negative control experiment was performed (data not shown).

Protein sample purification

Brush border membrane vesicles (BBMVs) and cortical membranes were prepared from intestinal and kidney samples using the Ca^{2+} precipitation method and used for immunoblotting analyses as described previously (30, 31).

Immunoblotting

Protein samples were incubated in sample buffer containing 2-mercaptoethanol at room temperature for 15 min and then subjected to 8% sodium dodecyl sulfate-polyacrylamide gel electrophoresis. Separated proteins were transferred by electrophoresis to Immobilon®-P polyvinylidene difluoride membranes (Millipore, Billerica, MA, USA). Membranes were then incubated with diluted antibodies. Signals were detected using Immobilon® Western Chemiluminescent HRP Substrate (Millipore).

Immunofluorescence staining

Rat kidney and intestine tissue samples were fixed in 4% paraformaldehyde solution (pH 7.2) overnight at 4℃. Samples were then washed with phosphate-buffered saline, cryoprotected with 30% sucrose at 4℃, embedded in OCT compound (Miles), and frozen in hexane at -80℃. Frozen sections (5 μm thick) were transferred to MAS-coated slides (Matsunami Glass IND, Ltd.) and air-dried. Frozen sections were incubated with primary antibody overnight at 4℃. Sections were then incubated with Alexa Fluor 488 anti-rabbit or anti-mouse antibody (Molecular Probes) and Alexa Fluor 568 anti-mouse or anti-rabbit antibody (Molecular Probes) for 60 min at room temperature. Sections were mounted with Dapi Fluoromount GTM (Southern Biotech).

Antibodies

Rabbit anti-NaPi-2a, NaPi-2b, and NaPi-2c polyclonal antibodies were generated as previously described (31) and used for immunoblotting and immunofluorescence staining (31). Mouse anti-actin monoclonal antibody (Millipore) was used as an internal control. Horseradish peroxidase (HRP)-conjugated anti-rabbit or anti-mouse IgG was used as a secondary antibody (Jackson Immuno Research Laboratories, Inc, West Grove, PA, USA). Antibody dilutions used for immunoblotting were as follows : NaPi-2a (1 : 25,000), NaPi-2b (1 : 2,000), NaPi-2c (1 : 4,000), Pit-1 (Genetex inc, CA, USA, 1 : 1,500), Xpr1 (PROTEINTECH, 1 : 2000), NHE3 (Millipore, 1 : 6,000), and actin (1 : 100,000). Antibody dilutions used for immunofluorescence staining were as follows : NaPi-2a (1 : 500), NaPi-2b, NaPi-2c (1 : 300), NHE3 (Millipore, 1 : 500), and villin (Millipore, 1 : 200).

Preparation of rat jejunal tissue and Pi flux experiment

The ^{32}Pi flux experiment was performed according to previously described methods with minor modifications (32, 33). Rat jejunal tissues were isolated, sectioned longitudinally, and opened. The lumen of the jejunum was washed with Ringer solution (124 mM NaCl, 0.4 mM KH_2PO_4, 1.6 mM K_2HPO_4, 21 mM $NaHCO_3$, 5 mM glucose, 1 mM $MgCl_2$, 1.3 mM Ca-gluconate, 2 μM Indomethacin, pH 7.4). The muscular layer was removed by peeling. The remaining epithelial surface was placed in a diffusion chamber. The two sides of the membrane were filled with Ringer solution under bubbling with 5% vol/vol CO_2 and 95% vol/vol O_2. The temperature in the chamber was maintained at 37℃ during all experiments.

A control buffer (140 mM NaCl, 5.4 mM KCl, 1 mM $MgCl_2$, 1.2 mM $CaCl_2$, and 10 mM glucose, pH 6.0) was used with continuous bubbling with 5% vol/vol CO_2 and 95% vol/vol O_2. In Na-independent experiments, NaCl was replaced with an equivalent amount of KCl. At 15 mins after placement of the jejunal segment in the chamber, a substrate solution was added to the mucosal side. To evaluate the inhibitory effect of the study drugs, EOS789 (50 μM) and phosphonoformic acid (PFA ; 10 mM,

Table 1. Primers used for quantitative PCR

Primer name	Sense sequence	Antisence sequence
CYP27B1	GAGCAAACTCCAGGAAGCAG	TGAGGAATGATCAGGAGAGG
CYP24A1	TGGGAAGATGATGGTGACCC	TCGATGCAGGGCTTGACTG
FGF23	GCAACATTTTTGGATCGTATCA	GATGCTTCGGTGACAGGTAGA
PTH	TTGTCTCCTTACCCAGGCAGAT	CTTCTTGGTGGGCCTCTGGTAAC
NaPi-2a	GAGGAGCAAAAGCCAGAG	AGGGAGCAGACAAAGAGG
NaPi-2b	CCTGGGACCTGCCTGAACT	CAATCCCCTGGAAAATGCAG
NaPi-2c	AAGGACAATGTGGTGCTGTC	ACCATGCTGACCACGATAGAG
Pit-1	CCCATGGACCTGAAGGAGGA	GCCACTGGAGTTGATCTGGT
Pit-2	GTGGATGGAACTCGTCAAG	CAGGATGAACAGCACACC
Xpr1	ATGAGAGTAAGGGCCTGTTG	GGCACTGGATGAATCGAAGC
NHE3	GCATAGTGTCCTTCTTCGTG	GGCTCGATGATACGCACATG
CLDN2	ACAGCACTGGCATCACCCA	GCGAGGACATTGCACTGGAT
CLDN3	ACCGCACCATCACCACTAC	CGTGGCGTCTGTAACCATC
CLDN7	TGGCAGGTCTTGCTGCTTTG	TGCCCAGCCGATAAAGATGG
CLDN12	TGCTCTTCTGCTGTTTGTTTGG	TGATGAATAGGGCTGTGAGTAA
CLDN15	GGCATGGTTGCTATCTCATG	CAGAGCCCAGTTCATACTTG
GAPDH	CTGCACCACCAACTGCTTAGC	CATCCACAGTCTTCTGGGTG

Sigma-Aldrich, St. Louis, MO, USA) were added to the substrate solution, respectively. The substrate solution was prepared to a Pi of 0.1 mM for the intercellular phosphate transport experiment and 10 mM for the paracellular transport experiment. ^{32}P (10 μCi/ml) was applied to the apical side of the membrane.

Statistical analyses

Data were expressed as the mean ± SE. Differences between multiple groups were compared using analysis of variance followed by the Scheffe test. Differences between two experimental groups were compared using analysis of variance followed by Student's t test. P-values less than 0.05 were considered statistically significant.

RESULTS

Comparison of $^{33}PO4$ balance in rats treated with EOS789 or lanthanum carbonate

In the present study, the effect of EOS789 on intestinal and renal phosphate transporters was compared to lanthanum carbonate (LC). To determine the dose of LC that is equivalent to 0.15% EOS789, rats were fed a food mixture containing ^{33}P and varying doses of LC. The fecal ^{33}P excretion rate was significantly increased in EOS789 at 0.15% and LC at 1.50% and 3.00% compared to Control (Figure 2A). The urinary ^{33}P excretion rate was significantly decreased in EOS789 at 0.15% and LC at 1.50% and 3.00% compared to Control (Figure 2 B). The serum ^{33}P radioactivity was similar to EOS789 and LC compared to Control (Figure 2C). Changes in fecal ^{33}P excretion rate, urinary ^{33}P excretion rate, and blood ^{33}P activity in response to LC dosage are shown in Figs. 2D-2F. The dose of LC with the same inhibitory effect as 0.15% EOS789 on fecal ^{33}P excretion was 1.74% LC.

Phosphate metabolism in normal rats after treatment with EOS789 or lanthanum carbonate

No differences in plasma calcium concentrations or fecal calcium excretion were observed between groups during the experimental period (Figure 3A, 3B). Urinary calcium excretion was significantly higher in the LC group compared to the Control group, and a trend toward increased urinary calcium excretion

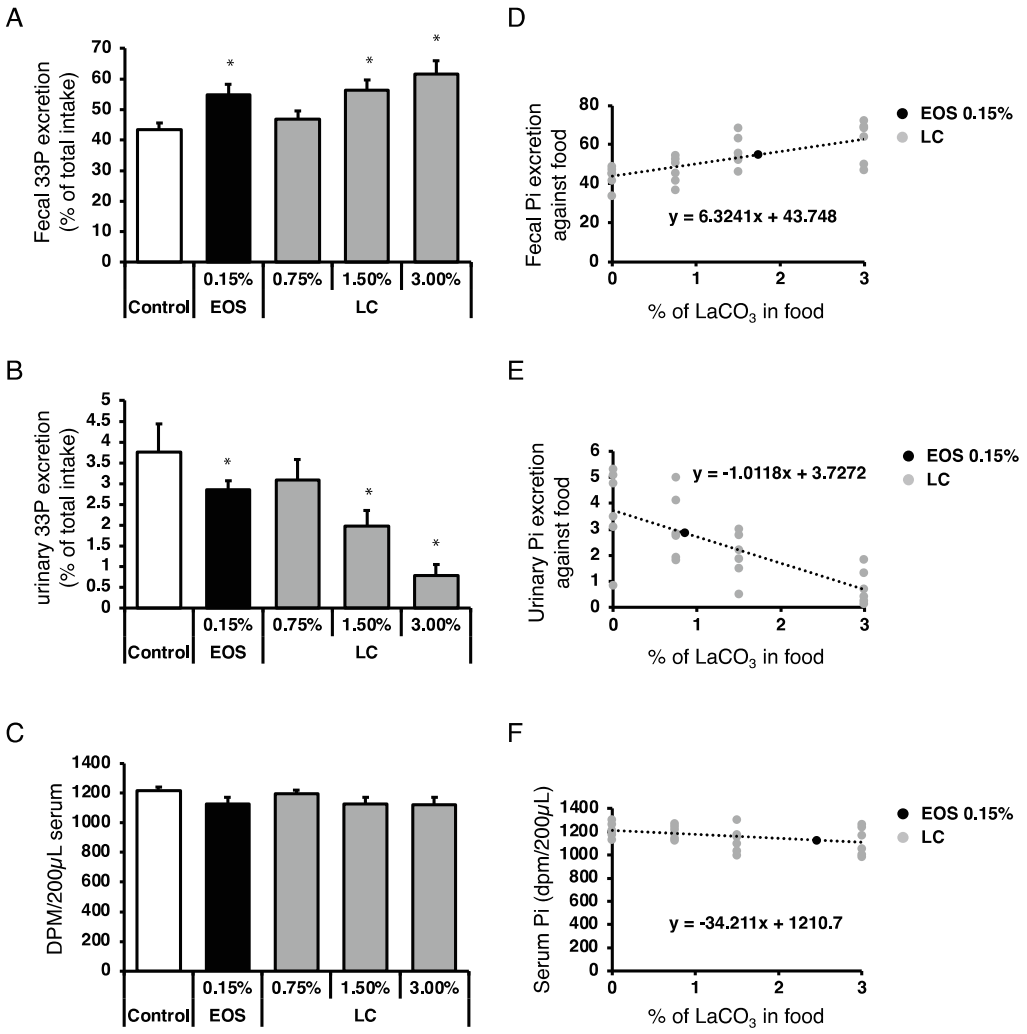

Figure 2. Comparison of $^{33}PO4$ balance in rats treated with EOS789 or lanthanum carbonate
(A) Fecal ^{33}P excretion rate. (B) Urinary ^{33}P excretion rate. (C) Serum ^{33}P radioactivity. (D) Changes in fecal ^{33}P excretion rate, (E) urinary ^{33}P excretion rate and (F) serum ^{33}P radioactivity in response according to lanthanum carbonate dose. Data are presented as mean ± SE. *$p < 0.05$ vs Control group.
EOS, EOS789 ; LC, lanthanum carbonate.

was observed in the EOS789 group compared to the Control group (Figure 3C). Plasma phosphate levels were significantly lower in the LC group compared to the Control group on day 3, with no difference in plasma phosphate levels observed between the EOS789 and Control groups (Figure 3D). Fecal phosphate excretion was significantly increased in the EOS789 and LC groups compared to the Control group on days 2 and 3 (Figure 3E). Urinary phosphate excretion was significantly decreased in both the EOS789 and LC groups compared to the Control group on days 2 and 3 (Figure 3F). No differences in serum sodium, potassium, chloride ion, or creatinine concentrations were observed between the EOS789 and LC groups compared to the Control group on day 3 (Table 2). Serum $1,25(OH)_2D_3$ levels were significantly increased in both the EOS789 and LC groups compared to the Control group (Figure 4A). Serum FGF23 levels were significantly decreased in both the EOS789 and LC groups

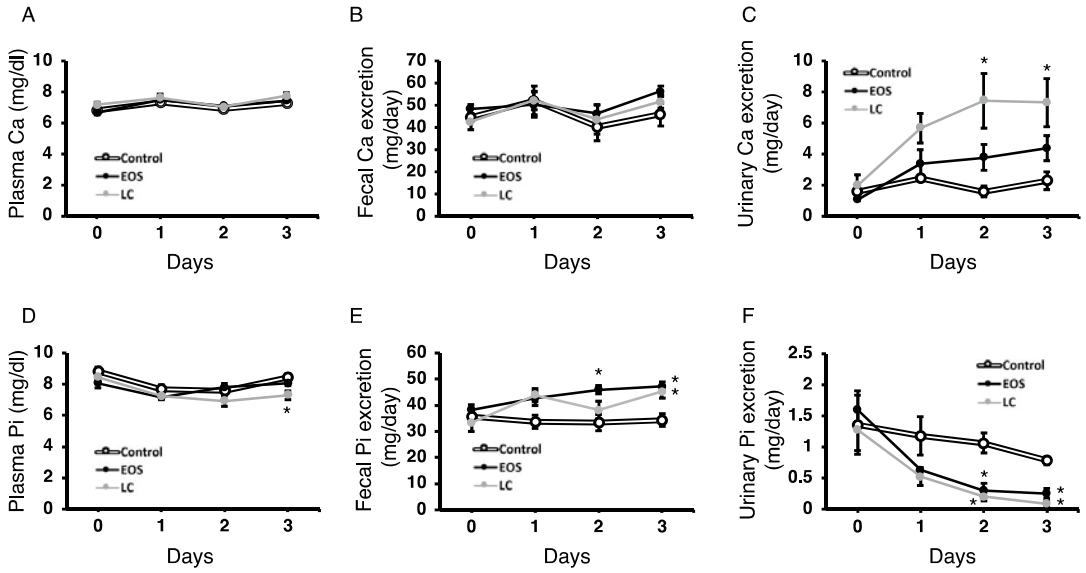

Figure 3. Physiological data in rats treated with EOS789
(A) Plasma calcium (Ca) concentration. (B) Fecal Ca excretion. (C) Urinary Ca excretion. (D) Plasma phosphate (Pi) concentration. (E) Fecal Pi excretion. (F) Urinary Pi excretion. Data are presented as mean ± SE (n = 4). *$p < 0.05$ vs Control group. EOS, EOS789 ; LC, lanthanum carbonate.

Table 2. Serological analyses

	Control	EOS	LC
CRE (mg/dL)	0.33 ± 0.01	0.31 ± 0	0.31 ± 0.02
UN (mg/dL)	11.2 ± 0.7	12.5 ± 1.4	12.5 ± 0.8
TP (g/dL)	4.92 ± 0.01	4.80 ± 0.11	4.83 ± 0.08
ALB (g/dL)	3.82 ± 0.08	3.72 ± 0.07	3.78 ± 0.05
Na-S (mmol/L)	147.3 ± 1.0	146.6 ± 1.3	144.5 ± 0.2
K-S (mmol/L)	4.32 ± 0.40	4.28 ± 0.22	3.92 ± 0.14
Cl-S (mmol/L)	110.9 ± 0.8	106.6 ± 4.4	106.7 ± 0.8
Fe (μg/dL)	128 ± 19	120 ± 3	142 ± 24
T-Bill (mg/dL)	0.06 ± 0	0.05 ± 0.01	0.05 ± 0
TBA (μmol/L)	37.3 ± 8.3	38.8 ± 5.8	31.4 ± 3.5
AST (U/L)	96 ± 3	96 ± 11	86 ± 5
ALT (U/L)	27 ± 2	28 ± 1	28 ± 1
ALPi (U/L)	260 ± 12	247 ± 9	220 ± 18
Mg (mg/dL)	2.3 ± 0.2	2.3 ± 0.1	2.1 ± 0
TG (mg/dL)	14 ± 1	16 ± 1	15 ± 1
T-CHOW (mg/dL)	69 ± 3	71 ± 2	68 ± 2
LDL (mg/L)	10 ± 1	9 ± 0	9 ± 0
GLU (mg/dL)	134 ± 10	118 ± 11	114 ± 3
NAG (U/L)	8.0 ± 0.4	8.0 ± 0.6	7.0 ± 0.4

EOS, EOS789 ; LC, lanthanum carbonate. Data are presented as mean ± SE (n = 4).

compared to the Control group (Figure 4B). However, plasma PTH levels were significantly lower in the LC group compared to the Control group, whereas no difference in plasma PTH levels was observed between the EOS789 and Control groups (Figure 4C). Real-time PCR measured mRNA expression levels of CYP27B1, CYP24A1, FGF23, and PTH (Figure 4D–G). Renal CYP27B1 mRNA levels were significantly higher in the LC group, but not the EOS789 group, compared to the Control group (Figure 4D). In contrast, renal CYP24A1 mRNA levels were significantly lower in the EOS789 group but not in the LC group compared to the Control group (Figure 4E). There was a trend toward lower FGF23 mRNA levels in bone tissues from the EOS789 and LC groups compared to the Control group (Figure 4F). There were no significant differences in PTH mRNA levels between the three groups (Figure 4G).

Intestinal phosphate transporter expression in normal rats after treatment with EOS789

We next measured intestinal Pi transporter mRNA and protein expression levels (Figure 5). No differences in NaPi-2b, Pit-1, or Pit-2 mRNA expression levels were observed between experimental groups (Figure 5A). Furthermore, no significant difference in NaPi-2b protein expression levels were observed between the Control and EOS789 groups (Figure 5B). However, showed significantly increased NaPi-2b protein levels were observed in the LC group compared to the Control and EOS789 groups (Figure 5B). Pit-1 protein levels were significantly lower in the EOS789 group, but not the LC group, compared to the Control group (Figure 5B). NaPi-2b protein levels were confirmed by immunofluorescence staining (Figure 5C).

Renal phosphate transporter expression in normal rats after treatment with EOS789

Renal expression of Pi transporters was then evaluated (Figure 6). No differences in NaPi-2a, NaPi-2c, Pit-1, or Pit-2 mRNA expression levels were observed between experimental groups (Figure 6A). No differences in NaPi-2a or NaPi-2c protein levels were observed between the Control and EOS789 groups ; however, higher NaPi-2a and NaPi-2c protein levels were observed in the LC group compared to the Control and EOS789 groups (Figure 6B). Significantly decreased Pit-1 protein levels were observed in the EOS789 and LC groups compared to the Control group (Figure 6B). NaPi-2a and NaPi-2c protein levels were confirmed by immunofluorescence staining (Figure 6C). We also examined the expression of Xpr1, which is thought to play a role in phosphate excretion on the basolateral side of the basement membrane (Figure 6D, E). No significant differences in renal Xpr1 mRNA expression or protein levels were observed between the experimental groups.

Intestinal NHE3 expression in normal rats after treatment with EOS789

Tenapanor inhibits NHE3 and reduces paracellular Pi permeability. EOS789 was developed as a Pi transporter-targeting compound ; however, no previous in vivo or in vitro studies have examined the effect of EOS789 on paracellular Pi transport. Accordingly, we examined intestinal NHE3 expression and mucosal-to-serosal Pi permeability in the present study. Intestinal NHE3 mRNA expression and protein levels were examined (Figure 7). No significant differences in NHE3 mRNA expression were observed between the experimental groups

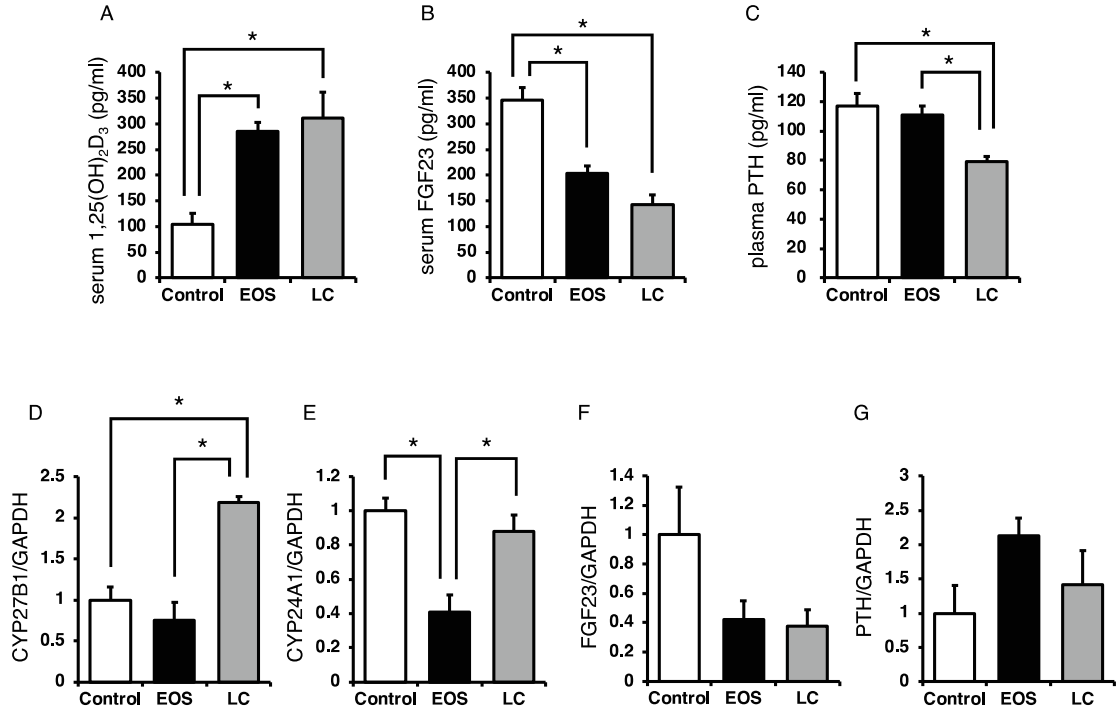

Figure 4. Vitamin D and phosphaturic hormone levels in rats treated with EOS789
(A) Serum $1,25(OH)_2D_3$ concentration. (B) Serum FGF23 concentration. (C) Plasma PTH concentration. (D) Renal CYP27B1 mRNA expression. (E) Renal CYP24A1 mRNA expression. (F) Femur FGF23 mRNA expression. (G) Parathyroid PTH mRNA expression. Values are from tissues harvested after treatment with EOS789 for three days. mRNA expression levels were normalized to GAPDH. Data are presented as mean ± SE (n = 4). * $p < 0.05$. EOS, EOS789 ; LC, lanthanum carbonate.

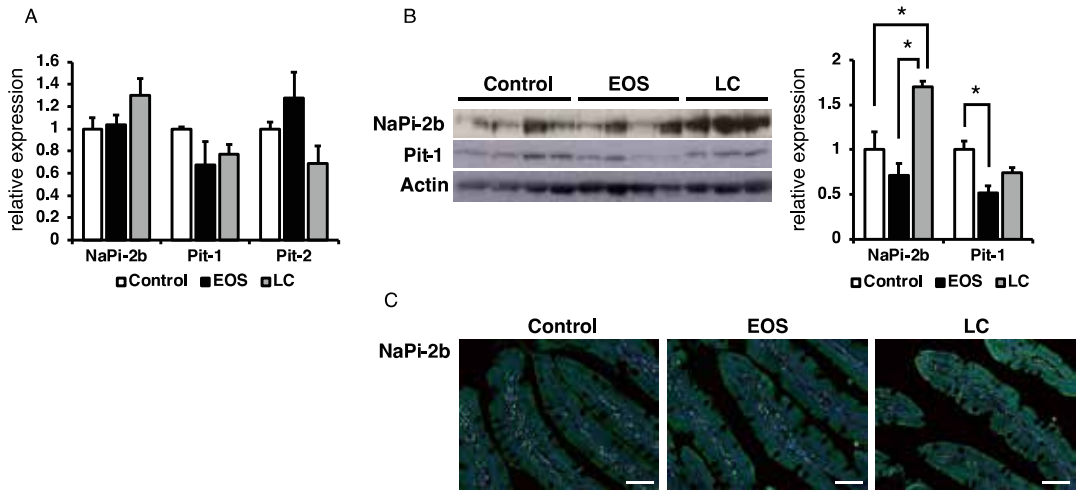

Figure 5. Intestinal phosphate transporter expression in rats treated with EOS789
Intestinal transporter expression in six-week-old Wistar rats treated with EOS789 or lanthanum carbonate for three days. (A) Upper intestinal Pi transporter mRNA expression (n = 4). (B) Western blot analysis of Pi transporter protein in upper intestinal BBMV (n = 3–4). mRNA expression levels were normalized to GAPDH. Protein levels were normalized to actin. (C) Representative image of immunofluorescence staining on a cross-sectional area of the intestine. Green, NaPi-2b ; blue, DAPI. Scale bar, 50 μm. * $p < 0.05$. EOS, EOS789 ; LC, lanthanum carbonate.

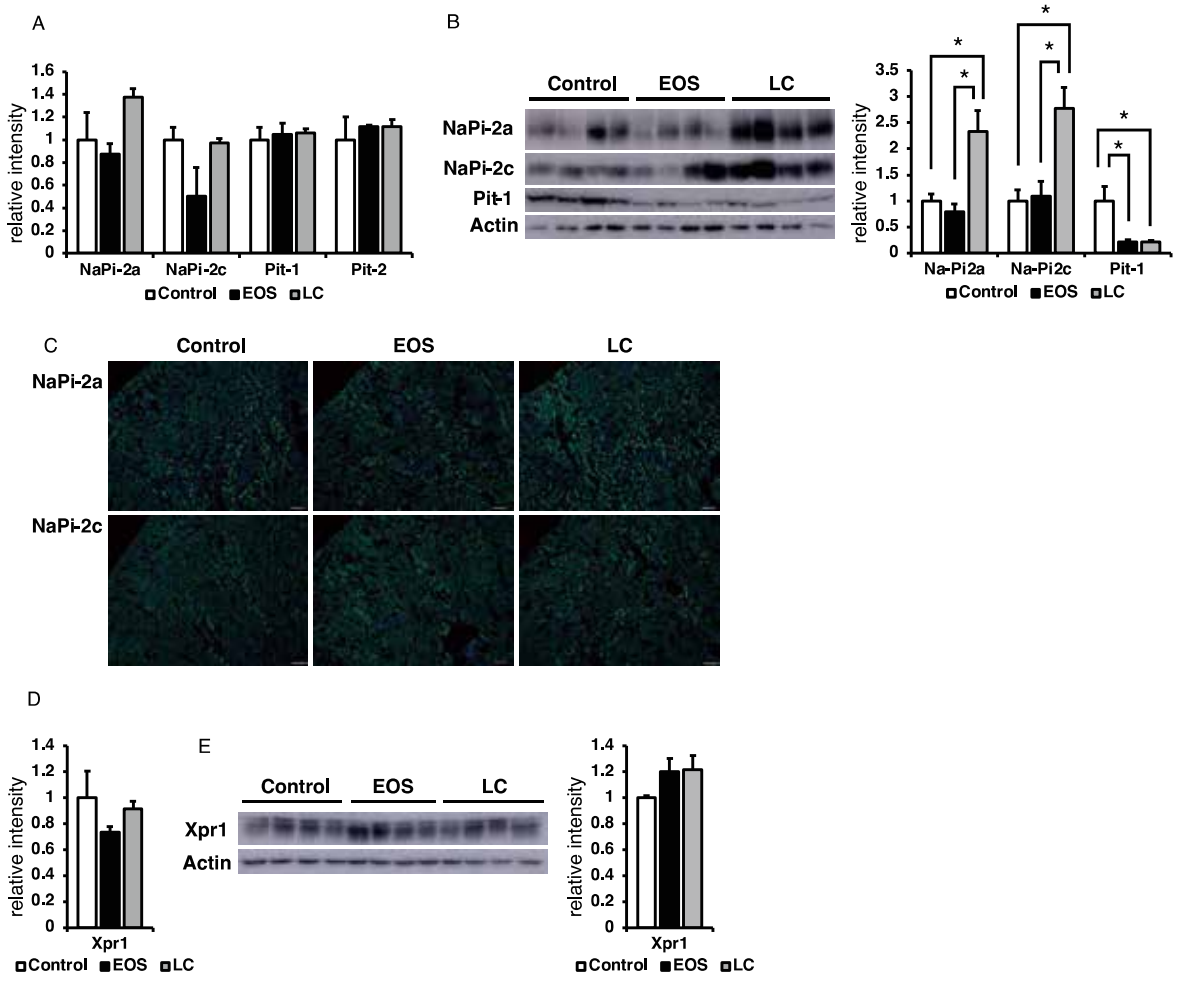

Figure 6. Renal phosphate transporter expression in rats treated with EOS789
Renal Pi transporter expression in six-week-old Wistar rats treated with EOS789 or lanthanum carbonate for three days. (A) Renal Pi transporter mRNA expression. (B) Western blot analysis of Pi transporter protein in renal BBMV. (C) Representative image of immunofluorescence staining on a cross-sectional area of the kidney. Green, NaPi-2a, or NaPi-2c ; blue, DAPI. Scale bar, 100 μm. (D) Renal Xpr1 mRNA expression. (E) Western blot analysis of Xpr1 protein in renal microsomes. mRNA expression levels were normalized to GAPDH. Protein levels were normalized to actin. Data are presented as mean ± SE (n = 4). * $p < 0.05$. EOS, EOS789 ; LC, lanthanum carbonate.

(Figure 7A). However, significantly reduced NHE3 protein levels were observed in the EOS789 group, but not the LC group, compared to the Control group (Figure 7B). Immunofluorescence staining confirmed the reduced NHE3 protein levels in the EOS789 group (Figure 7C). Figure 7D shows intestinal claudin mRNA levels were examined using real-time PCR. A significant decrease in claudin-12 mRNA expression was observed in the intestine of rats treated with LC. A significant decrease in claudin-15 mRNA expression was observed in the intestine of rats treated with EOS789.

Pi permeability in normal rats after treatment with EOS789

Finally, rat intestinal mucosal to serosal Pi permeability was measured at Pi concentrations of 0.1 mM and 10 mM. At a Pi concentration of 0.1 mM, Pi permeation was significantly lower in the absence of sodium compared to the presence of sodium (Figure 8A). Apical administration of EOS789 significantly reduced Pi permeation to similar levels observed with the absence of sodium or with the addition of PFA, an inhibitor of the Na+-dependent phosphate transporter (Figure 8A). At a Pi concentration of 10 mM, no significant differences in Pi permeation were observed between the presence and absence of sodium (Figure 8B). In contrast, EOS789 significantly reduced Pi permeation at a Pi concentration of 10 mM (Figure 8C). These results indicate that EOS789 may affect transcellular Pi transport in addition to paracellular Pi permeation in the small intestine of rats.

DISCUSSION

The present study investigated *in vivo* responses to EOS789, the novel drug, compared to a conventional Pi binder, LC, in rats. The results of the present study indicate EOS789 treatment may have greater efficacy in treating hyperphosphatemia compared to LC, albeit via different biological responses. Biochemical analyses demonstrated that fecal Pi excretion (Figure 3E) was significantly higher in the EOS789 group compared to the control group, with a significant decrease in urinary Pi excretion (Figure 3F) observed which likely represents a compensatory mechanism. Furthermore, the increased in vivo Pi requirements in the EOS789 group may resulted in increased urinary calcium excretion (Figure 3C), increased blood active vitamin D (Figure 4A), and decreased FGF23 (Figure 4B). However, EOS789 appeared to have less a potent inhibitory effect on Pi absorption compared to LC in vivo. Indeed, significantly decreased blood Pi levels (Figure 3D), increased urinary calcium excretion (Fig-

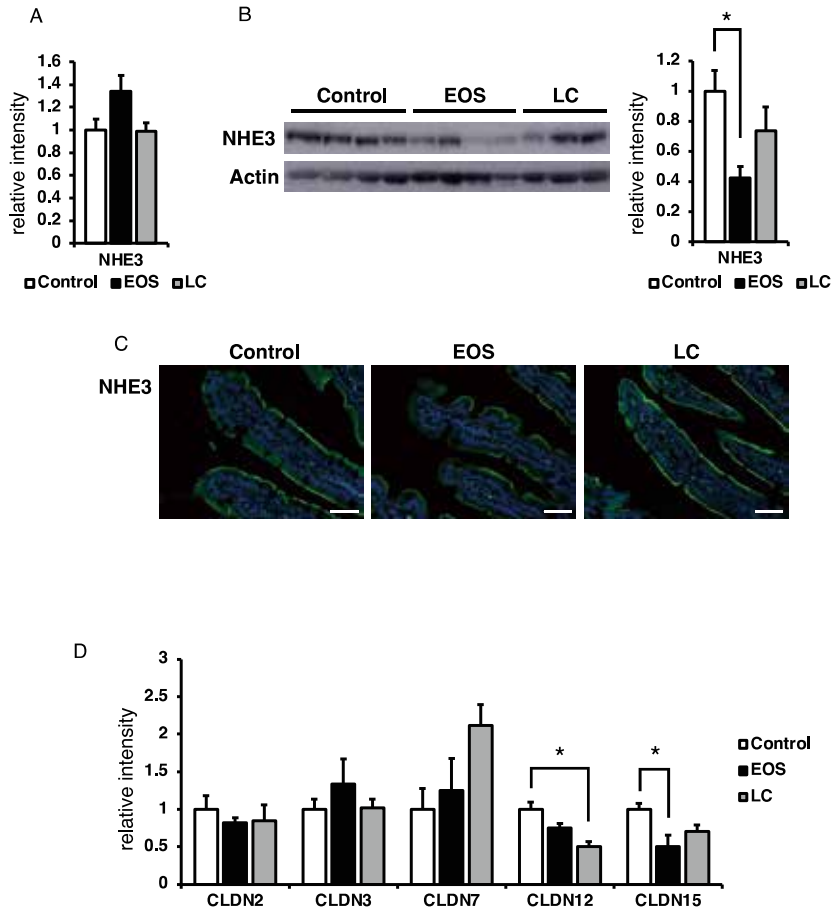

Figure 7. Response of intestinal NHE3 and claudin expression in normal rats after administration of EOS789
Six-week-old Wistar rats were treated with EOS789 or lanthanum carbonate for three days. (A) Intestinal NHE3 mRNA expression (n = 4). mRNA expression levels were normalized to GAPDH. (B) Western blot analysis of NHE3 protein in upper intestinal BBMV (n = 3–4). Protein levels were normalized to actin. (C) Representative image of immunofluorescence staining for NHE3 on a cross-sectional area of the intestine. Green, NHE3 ; blue, DAPI. Scale bar, 50 μm. (D) Intestinal claudin mRNA expression (n = 4). mRNA expression levels were normalized to GAPDH. Data are presented as mean ± SE. * $p < 0.05$. EOS, EOS789 ; LC, lanthanum carbonate.

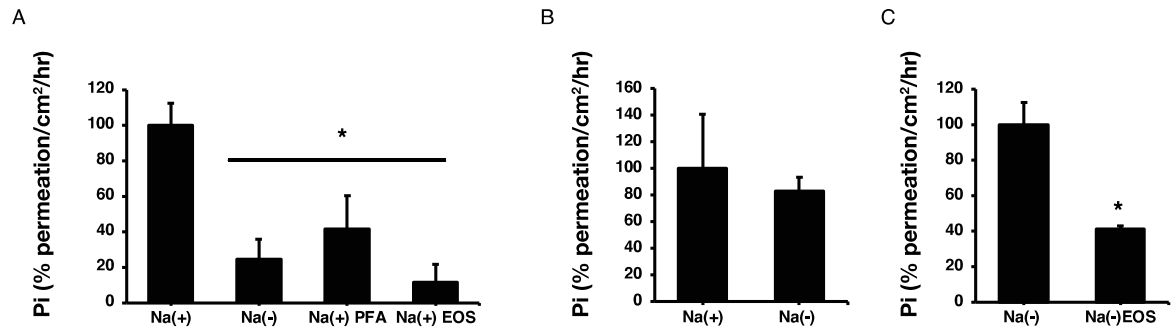

Figure 8. Pi permeability
The ^{32}Pi permeability experiment was performed on jejunal tissue from normal rats fed a standard rat chow diet. Mucosal to serosal Pi permeability in rat intestinal tissue was measured at Pi concentrations of 0.1 mM (A) or 10 mM (B, C). Data are presented as mean ± SE. *$p < 0.05$. EOS, EOS789 ; PFA, phosphonoformic acid.

ure 3C), and decreased PTH levels (Figure 4C) were observed in the LC group compared to the control group. Regarding the expression of intestinal and renal Pi transporters, a significant increase in intestinal NaPi-2b and renal NaPi-2a and NaPi-2c protein levels was observed in the LC group but not in EOS789, compared to the Control group (Figure 5B, Figure 6B). Decreased PTH levels, increased urinary calcium excretion, and increased renal NaPi-2a protein levels have previously been reported following treatment with sevelamer hydrochloride, a non-calcium phosphate binder (34). Accordingly, Pi binders, and EOS789 appear to induce differing in vivo responses.

The differences in the effects of EOS789 and LC on Pi metabolism are thought to be dependent on drug properties. Pi adsorbents (LC) bind dietary Pi in the intestinal lumen and are excreted in feces, thereby reducing the luminal Pi concentration. On the other hand, EOS789 inhibits Pi absorption, and increases luminal Pi concentration. These differences are thought to result in distinct physiological responses to Pi. Previous studies have reported that NaPi-2b levels are affected by dietary phosphorus content, with levels particularly increased during phosphorus restriction (8, 35). As Pi concentrations in the intestinal lumen following treatment with Pi binders are similar to during phosphorus restriction, Pi binders may contribute to increased NaPi-2b expression. Indeed, a significant increase in NaPi-2b expression was observed in the LC group in the present study (Figure 5B). Increased NaPi-2b expression promotes intestinal Pi absorption and is considered a cause of resistance to Pi binders. However, EOS789 may not affect NaPi-2b expression as it creates a high Pi environment in the intestinal lumen.

A further novel finding of the present study is that treatment with EOS789 suppresses intestinal NHE3 protein levels. NHE3 mediates Na^+ absorption in the intestine and kidneys (36). Tenapanor (AZD1722, RDX5791) is an inhibitor of NHE3 that is minimally absorbed from the gastrointestinal tract (37). Recent studies have reported that tenapanor alters Pi homeostasis by potentially reducing intestinal paracellular Pi transport and reducing expression of intestinal NaPi-2b (28). Pre-clinical and clinical studies have reported that tenapanor reduces plasma Pi levels in hemodialysis patients with hyperphosphatemia (29, 38-48).

Intestinal NHE3 regulates small intestinal calcium absorption, with the concentration of active vitamin D an important regulator of intestinal NHE3 levels (49). In the present study, plasma levels of active vitamin D were increased in both the EOS789 and LC groups (Figure 4A). Therefore, differences in active vitamin D concentrations do not appear to result in NHE3 suppression. NHE3 expression and activity are regulated by short-term and long-term mechanisms (50, 51), with many factors posited to contribute to the regulation of intestinal NHE3 (49). Further detailed investigations are required to elucidate the mechanism of action underlying the effect of EOS789 on decreasing intestinal NHE3 levels.

As EOS789 significantly reduced NHE3 protein levels (Figure 7B), we investigated intestinal Pi transcellular and paracellular transport. The results of the present study indicate that EOS789 may inhibit transcellular Pi transport in addition to paracellular transport. Tight junctions are the most apical component of the junctional complex, providing a form of cell-cell adhesion in enterocytes and playing a critical role in regulating paracellular barrier permeability (52). Hashimoto *et al*. reported that claudin-3 plays a pivotal role in the regulation of paracellular permeability to Pi (53). We also reported that claudin-2, -12, and -15 protein levels were significantly decreased in a NaPi-2b conditional KO mouse model (12). In the present study, mRNA expression levels of several claudins were examined, with a significant decrease in claudin-15 mRNA expression observed in the intestine of rats treated with EOS789 (Figure 7D). Claudin-15 is a tight junction protein that has been identified as an essential regulator of paracellular Na^+ flux and transcellular nutrient absorption. Inhibition of molecules involved in sodium transport, such as NHE3, and claudin-15, affects intestinal Pi permeability. However, we did not evaluate sodium transport in the present study. Further studies of the role of claudin-15 in intestinal Pi absorption are warranted.

Finally, we observed differing physiological effects of LC and EOS789 on phosphorus metabolism. EOS789 inhibits intestinal phosphate absorption with a mechanism of action that differs from phosphate binders. We confirmed the inhibitory effects of EOS789 on intestinal transcellular and paracellular Pi transport. EOS789 treatment may benefit patients who are ineffectively treated with Pi binders. Furthermore, the combined use of Pi binders and EOS789 may allow tighter restriction of Pi levels.

CONFLICT OF INTERESTS

Tanifuji K., Shiozaki Y., Koike M., Uga M., Komiya A., Miura M., Higashi A., Shimohata T., Takahashi A., Ishizuka N., Hayashi H., Miyamoto K., Segawa H. have declared no conflicts of interest related to the present study. Ichida Y., Ohtomo S., and Horiba N. are employees of Chugai Pharmaceutical Co., Ltd.

ACKNOWLEDGMENTS

This study was supported by the Support Center for Advanced Medical Sciences, Tokushima University Graduate School of Biomedical Sciences. This work was supported by JSPS KAKENHI Grants (JP20K08637 to K.M., JP21H03375 to H.S.)

ANIMAL RIGHTS

Rats were handled in accordance with the Guidelines for Animal Experimentation of Tokushima University School of Medicine and with the Guidelines for the Care and Use of Laboratory Animals at Chugai Pharmaceuticals. This article does not contain any studies involving human participants.

REFERENCES

1. Musgrove J, Wolf M : Regulation and Effects of FGF23 in Chronic Kidney Disease. Annu Rev Physiol 82 : 365-90, 2020
2. Doshi SM, Wish JB : Past, Present, and Future of Phosphate Management. Kidney Int Rep 7 : 688-98, 2022
3. Chan M, Kelly J, Tapsell L : Dietary Modeling of Foods for Advanced CKD Based on General Healthy Eating Guidelines : What Should Be on the Plate? Am J Kidney Dis 69 : 436-50, 2017
4. Duque EJ, Elias RM, Moysés RMA : Phosphate balance during dialysis and after kidney transplantation in patients with chronic kidney disease. Curr Opin Nephrol Hypertens 31 : 326-31, 2022
5. Vallée M, Weinstein J, Battistella M, Papineau R, Moseley D, Wong G : Multidisciplinary Perspectives of Current Approaches and Clinical Gaps in the Management of Hyperphosphatemia. Int J Nephrol Renovasc Dis 14 : 301-11, 2021
6. Ketteler M, Liangos O, Biggar PH : Treating hyperphosphatemia - current and advancing drugs. Expert Opin Pharmacother 17 : 1873-9, 2016
7. Copland M, Komenda P, Weinhandl ED, McCullough PA, Morfin JA : Intensive Hemodialysis, Mineral and Bone Disorder, and Phosphate Binder Use. Am J Kidney Dis 68 : S24-S32, 2016
8. Hernando N, Gagnon K, Lederer E : Phosphate Transport in Epithelial and Nonepithelial Tissue. Physiol Rev 101 : 1-35, 2021
9. Marks J : The role of SLC34A2 in intestinal phosphate absorption and phosphate homeostasis. Pflugers Arch 471 : 165-73, 2019
10. Jacquillet G, Unwin RJ : Physiological regulation of phosphate by vitamin D, parathyroid hormone (PTH) and phosphate (Pi). Pflugers Arch 471 : 83-98, 2019
11. Kaneko I, Tatsumi S, Segawa H, Miyamoto KI : Control of phosphate balance by the kidney and intestine. Clin Exp Nephrol 21 : 21-6, 2017
12. Ikuta K, Segawa H, Sasaki S, Hanazaki A, Fujii T, Kushi A, Kawabata Y, Kirino R, Sasaki S, Noguchi M, Kaneko I, Tatsumi S, Ueda O, Wada NA, Tateishi H, Kakefuda M, Kawase Y, Ohtomo S, Ichida Y, Maeda A, Jishage KI, Horiba N, Miyamoto KI : Effect of Npt2b deletion on intestinal and renal inorganic phosphate (Pi) handling. Clin Exp Nephrol 22 : 517-28, 2018
13. Ohi A, Hanabusa E, Ueda O, Segawa H, Horiba N, Kaneko I, Kuwahara S, Mukai T, Sasaki S, Tominaga R, Furutani J, Aranami F, Ohtomo S, Oikawa Y, Kawase Y, Wada NA, Tachibe T, Kakefuda M, Tateishi H, Matsumoto K, Tatsumi S, Kido S, Fukushima N, Jishage K, Miyamoto K : Inorganic phosphate homeostasis in sodium-dependent phosphate cotransporter Npt2b$^{+/-}$ mice. Am J Physiol Renal Physiol 301 : F1105-13, 2011
14. Schiavi SC, Tang W, Bracken C, O'Brien SP, Song W, Boulanger J, Ryan S, Phillips L, Liu S, Arbeeny C, Ledbetter S, Sabbagh Y : Npt2b deletion attenuates hyperphosphatemia associated with CKD. J Am Soc Nephrol 23 : 1691-700, 2012
15. Sabbagh Y, O'Brien SP, Song W, Boulanger JH, Stockmann A, Arbeeny C, Schiavi SC : Intestinal npt2b plays a major role in phosphate absorption and homeostasis. J Am Soc Nephrol 20 : 2348-58, 2009
16. Ushiki Y, Kawabe K, Yamamoto-Okada K, Uneuchi F, Asanuma Y, Yamaguchi C, Ohta H, Shibata T, Abe T, Okumura-Kitajima L, Kosai Y, Endo M, Otake K, Munetomo E, Takahashi T, Kakinuma H : Design, synthesis and biological evaluation of novel 1H-pyrazole-4-carbonyl-4,5,6,7-tetrahydrobenzo [b]thiophene derivatives as gut-selective NaPi2b inhibitors. Bioorg Med Chem Lett 59 : 128572, 2022
17. Ushiki Y, Kawabe K, Yamamoto-Okada K, Uneuchi F, Asanuma Y, Yamaguchi C, Ohta H, Shibata T, Abe T, Okumura-Kitajima L, Kosai Y, Endo M, Otake K, Munetomo E, Takahashi T, Kakinuma H : Design, synthesis and biological evaluation of novel pyridine derivatives as gutselective NaPi2b inhibitors. Bioorg Med Chem Lett 65 : 128700, 2022
18. Ushiki Y, Kawabe K, Yamamoto-Okada K, Uneuchi F, Asanuma Y, Yamaguchi C, Ohta H, Shibata T, Abe T, Okumura-Kitajima L, Kosai Y, Endo M, Otake K, Munetomo E, Takahashi T, Kakinuma H : Design, synthesis and biological evaluation of novel indole derivatives as gut-selective NaPi2b inhibitors. Bioorg Med Chem 66 : 116783, 2022
19. Maemoto M, Hirata Y, Hosoe S, Ouchi J, Uchii M, Takada H, Akizawa E, Yanagisawa A, Shuto S : Development of potent non-acylhydrazone inhibitors of intestinal sodium-dependent phosphate transport protein 2b (NaPi2b). Bioorg Med Chem 71 : 116944, 2022
20. Maemoto M, Hirata Y, Hosoe S, Ouchi J, Narushima K, Akizawa E, Tsuji Y, Takada H, Yanagisawa A, Shuto S : Discovery of Gut-Restricted Small-Molecule Inhibitors of Intestinal Sodium-Dependent Phosphate Transport Protein 2b (NaPi2b) for the Treatment of Hyperphosphatemia. J Med Chem 65 : 1946-60, 2022
21. Matsuo A, Negoro T, Seo T, Kitao Y, Shindo M, Segawa H, Miyamoto K : Inhibitory effect of JTP-59557, a new triazole derivative, on intestinal phosphate transport in vitro and in vivo. Eur J Pharmacol 517 : 111-9, 2005
22. Maruyama S, Marbury TC, Connaire J, Ries D, Maxwell W, Rambaran C : NaPi-IIb Inhibition for Hyperphosphatemia in CKD Hemodialysis Patients. Kidney Int Rep 6 : 675-84, 2021
23. Larsson TE, Kameoka C, Nakajo I, Taniuchi Y, Yoshida S, Akizawa T, Smulders RA : NPT-IIb Inhibition Does Not Improve Hyperphosphatemia in CKD. Kidney Int Rep 3 : 73-80, 2018
24. Ichida Y, Hosokawa N, Takemoto R, Koike T, Nakatogawa T, Hiranuma M, Arakawa H, Miura Y, Azabu H, Ohtomo S, Horiba N : Significant Species Differences in Intestinal Phosphate Absorption between Dogs, Rats, and Monkeys. J Nutr Sci Vitaminol (Tokyo) 66 : 60-7, 2020
25. Tsuboi Y, Ichida Y, Murai A, Maeda A, Iida M, Kato A, Ohtomo S, Horiba N : EOS789, panphosphate transporter inhibitor, ameliorates the progression of kidney injury in

anti-GBM-induced glomerulonephritis rats. Pharmacol Res Perspect 10 : e00973, 2022
26. Tsuboi Y, Ohtomo S, Ichida Y, Hagita H, Ozawa K, Iida M, Nagao S, Ikegami H, Takahashi T, Horiba N : EOS789, a novel pan-phosphate transporter inhibitor, is effective for the treatment of chronic kidney disease-mineral bone disorder. Kidney Int 98 : 343-54, 2020
27. Hill Gallant KM, Stremke ER, Trevino LL, Moorthi RN, Doshi S, Wastney ME, Hisada N, Sato J, Ogita Y, Fujii N, Matsuda Y, Kake T, Moe SM : EOS789, a broad-spectrum inhibitor of phosphate transport, is safe with an indication of efficacy in a phase 1b randomized crossover trial in hemodialysis patients. Kidney Int 99 : 1225-33, 2021
28. King AJ, Siegel M, He Y, Nie B, Wang J, Koo-McCoy S, Minassian NA, Jafri Q, Pan D, Kohler J, Kumaraswamy P, Kozuka K, Lewis JG, Dragoli D, Rosenbaum DP, O'Neill D, Plain A, Greasley PJ, Jonsson-Rylander AC, Karlsson D, Behrendt M, Stromstedt M, Ryden-Bergsten T, Knopfel T, Pastor Arroyo EM, Hernando N, Marks J, Donowitz M, Wagner CA, Alexander RT, Caldwell JS : Inhibition of sodium/hydrogen exchanger 3 in the gastrointestinal tract by tenapanor reduces paracellular phosphate permeability. Sci Transl Med 10 : 2018
29. Block GA, Rosenbaum DP, Leonsson-Zachrisson M, Astrand M, Johansson S, Knutsson M, Langkilde AM, Chertow GM : Effect of Tenapanor on Serum Phosphate in Patients Receiving Hemodialysis. J Am Soc Nephrol 28 : 1933-42, 2017
30. Furutani J, Segawa H, Aranami F, Kuwahara S, Sugano M, Bannai K, Yamato H, Ito M, Miyamoto K : Dietary inorganic phosphorus regulates the intestinal peptide transporter PepT1. J Ren Nutr 23 : e11-20, 2013
31. Segawa H, Yamanaka S, Ito M, Kuwahata M, Shono M, Yamamoto T, Miyamoto K : Internalization of renal type IIc Na-Pi cotransporter in response to a high-phosphate diet. Am J Physiol Renal Physiol 288 : F587-96, 2005
32. Eto N, Tomita M, Hayashi M : NaPi-mediated transcellular permeation is the dominant route in intestinal inorganic phosphate absorption in rats. Drug Metab Pharmacokinet 21 : 217-21, 2006
33. Knöpfel T, Himmerkus N, Günzel D, Bleich M, Hernando N, Wagner CA : Paracellular transport of phosphate along the intestine. American Journal of Physiology-Gastrointestinal and Liver Physiology 317 : G233-G41, 2019
34. Nagano N, Miyata S, Obana S, Eto N, Fukushima N, Burke SK, Wada M : Renal mineral handling in normal rats treated with sevelamer hydrochloride (Renagel), a noncalcemic phosphate binder. Nephron 89 : 321-8, 2001
35. Segawa H, Kaneko I, Yamanaka S, Ito M, Kuwahata M, Inoue Y, Kato S, Miyamoto K : Intestinal Na-P(i) cotransporter adaptation to dietary P(i) content in vitamin D receptor null mice. Am J Physiol Renal Physiol 287 : F39-47, 2004
36. Kovesdy CP, Adebiyi A, Rosenbaum D, Jacobs JW, Quarles LD : Novel Treatments from Inhibition of the Intestinal Sodium-Hydrogen Exchanger 3. Int J Nephrol Renovasc Dis 14 : 411-20, 2021
37. Johansson S, Rosenbaum DP, Knutsson M, Leonsson-Zachrisson M : A phase 1 study of the safety, tolerability, pharmacodynamics, and pharmacokinetics of tenapanor in healthy Japanese volunteers. Clinical and Experimental Nephrology 21 : 407-16, 2017
38. Lin T, Al-Makki A, Shepler B : Tenapanor : A new treatment option for hyperphosphatemia in end stage kidney disease. J Pharm Pharm Sci 25 : 77-83, 2022
39. Inaba M, Une Y, Ikejiri K, Kanda H, Fukagawa M, Akizawa T : Dose-Response of Tenapanor in Patients With Hyperphosphatemia Undergoing Hemodialysis in Japan-A Phase 2 Randomized Trial. Kidney Int Rep 7 : 177-88, 2022
40. Shigematsu T, Une Y, Ikejiri K, Kanda H, Fukagawa M, Akizawa T : Therapeutic Effects of Add-On Tenapanor for Hemodialysis Patients with Refractory Hyperphosphatemia. Am J Nephrol 52 : 496-506, 2021
41. Pergola PE, Rosenbaum DP, Yang Y, Chertow GM : A Randomized Trial of Tenapanor and Phosphate Binders as a Dual-Mechanism Treatment for Hyperphosphatemia in Patients on Maintenance Dialysis (AMPLIFY). J Am Soc Nephrol 32 : 1465-73, 2021
42. Akizawa T, Sato Y, Ikejiri K, Kanda H, Fukagawa M : Effect of Tenapanor on Phosphate Binder Pill Burden in Hemodialysis Patients. Kidney Int Rep 6 : 2371-80, 2021
43. Cozzolino M, Ketteler M, Wagner CA : An expert update on novel therapeutic targets for hyperphosphatemia in chronic kidney disease : preclinical and clinical innovations. Expert Opin Ther Targets 24 : 477-88, 2020
44. Block GA, Rosenbaum DP, Yan A, Greasley PJ, Chertow GM, Wolf M : The effects of tenapanor on serum fibroblast growth factor 23 in patients receiving hemodialysis with hyperphosphatemia. Nephrol Dial Transplant 34 : 339-46, 2019
45. Block GA, Rosenbaum DP, Yan A, Chertow GM : Efficacy and Safety of Tenapanor in Patients with Hyperphosphatemia Receiving Maintenance Hemodialysis : A Randomized Phase 3 Trial. J Am Soc Nephrol 30 : 641-52, 2019
46. Johansson S, Rosenbaum DP, Knutsson M, Leonsson-Zachrisson M : A phase 1 study of the safety, tolerability, pharmacodynamics, and pharmacokinetics of tenapanor in healthy Japanese volunteers. Clin Exp Nephrol 21 : 407-16, 2017
47. Johansson S, Leonsson-Zachrisson M, Knutsson M, Spencer AG, Labonte ED, Deshpande D, Kohler J, Kozuka K, Charmot D, Rosenbaum DP : Preclinical and Healthy Volunteer Studies of Potential Drug-Drug Interactions Between Tenapanor and Phosphate Binders. Clin Pharmacol Drug Dev 6 : 448-56, 2017
48. Block GA, Rosenbaum DP, Leonsson-Zachrisson M, Stefansson BV, Ryden-Bergsten T, Greasley PJ, Johansson SA, Knutsson M, Carlsson BC : Effect of Tenapanor on Interdialytic Weight Gain in Patients on Hemodialysis. Clin J Am Soc Nephrol 11 : 1597-605, 2016
49. Gill R, Nazir TM, Wali R, Sitrin M, Brasitus TA, Ramaswamy K, Dudeja PK : Regulation of rat ileal NHE3 by 1,25(OH)2-vitamin D3. Dig Dis Sci 47 : 1169-74, 2002
50. Nwia SM, Li XC, Leite APO, Hassan R, Zhuo JL : The Na(+)/H(+) Exchanger 3 in the Intestines and the Proximal Tubule of the Kidney : Localization, Physiological Function, and Key Roles in Angiotensin II-Induced Hypertension. Front Physiol 13 : 861659, 2022
51. Zachos NC, Tse M, Donowitz M : MOLECULAR PHYSIOLOGY OF INTESTINAL N+/H+EXCHANGE. Annual Review of Physiology 67 : 411-43, 2005
52. Lu Z, Ding L, Lu Q, Chen Y-H : Claudins in intestines. Tissue Barriers 1 : e24978, 2013
53. Hashimoto N, Matsui I, Ishizuka S, Inoue K, Matsumoto A, Shimada K, Hori S, Lee DG, Yasuda S, Katsuma Y, Kajimoto S, Doi Y, Yamaguchi S, Kubota K, Oka T, Sakaguchi Y, Takabatake Y, Hamano T, Isaka Y : Lithocholic acid increases intestinal phosphate and calcium absorption in a vitamin D receptor dependent but transcellular pathway independent manner. Kidney Int 97 : 1164-80, 2020